

7 Nanostructures at Solid/Liquid Interface

Li-Jun Wan* and Chun-Li Bai

*Institute of Chemistry, Chinese Academy of Sciences,
Beijing 100080, China*

1 INTRODUCTION

The advanced engineering for constructing a molecular electronic device requires various nano-size elements such as molecular line, molecular switch and diode. With the development of scanning probe techniques, particularly scanning tunneling microscopy (STM), scientists can, at atomic scale, find device-like characteristics in pre-existing structures, create new structures by atomic manipulation and try to apply them for industrial uses. Electrochemical techniques can be employed to construct atomic or molecular patterns, films and nanostructures on solid surface in electrolyte solutions. The electrochemical STM (ECSTM), combining electrochemistry and STM, can effectively work in electrolyte solution similarly as STM in UHV or ambient conditions and monitor the formation and transition process of molecule structure on the solid surface with the electrode potential.

The adsorption of ions and molecules on electrode surface is of special interest in the studies such as catalysis, corrosion, nano-engineering, underpotential deposition and surface coordination. By using self-assembled monolayer technique, Whitesides *et al.* (1991) prepared various two-dimensional molecular structures and examined their arrangements. Jung *et al.* (1996, 1997) identified the conformation of individual Cu-TBPP molecules on low-index surfaces of Au, Ag and Cu, and demonstrated a controlled positioning at room-temperature on Cu(100) surface. Fishlock *et al.* (2000) reported the manipulation of Br atoms at room temperature across a Cu(100) surface. Eigler *et al.* (1990, 1991), Strosio and Eigler (1991) have performed many striking researches of single molecule and produced the first “hand-built” atomic structure. Seven Xe atoms bonded together to form a linear chain on Ni(100) surface (Eigler and Schweizer, 1990). With STM they realized the motion of a single atom from substrate to tip as an atomic switch. Gimzewski *et al.* (1998) demonstrated rotation of a single molecule within a supermolecular bearing. It has been reviewed (Itaya, 1998) that the structures and electrochemical features of Cl⁻, Br⁻, I⁻, SO₄²⁻, S₂²⁻, CN⁻, SCN⁻ adlayers on both polycrystalline and single-crystal metal surfaces of Au, Pt, Cu, Ag, Pd, Rh and Ir were well issued. On the other hand, if a controlled reversible action of a molecule such as controlled molecular orientation and motion, could be achieved by the application of an electric signal, a functional molecular element might be

* Corresponding author. Tel & Fax: +86-10-62558934; Email: [wanlijun@infoc3.icas.ac.cn](mailto:wanjijun@infoc3.icas.ac.cn)

developed. Here, we report the result of controlling sulfur, which can be applied in the electrodeposition of well-defined semiconductor thin films, and organic molecules, 2,2'-bipyridine (bpy) and 1,3,5-triazine-2,4,6-trithiol (trithiol), on Cu(111) in HClO₄ solution by ECSTM. It is shown that the structure of the adsorption of sulfur is potential dependent with a well-ordered ($\sqrt{7} \times \sqrt{7}$)R19.1° structure at the potential of -0.32 V and a moiré pattern at the potential of -0.20 V, while the two organic molecules could take flat and vertical orientation on Cu(111) in response to the applied electrode potentials and the variation is completely potential dependent, reversible and stable. If considering the different states as one or zero, the molecules behave like a functional electronic device.

2 EXPERIMENTAL

A commercial Cu(111) single-crystal disk with a diameter of 10 mm (from MaTeck) was used as a working electrode for both electrochemical measurement and *in situ* STM observation. A homemade electrochemical cell containing a reversible hydrogen electrode (RHE) in 0.1 M HClO₄ and a Pt counter electrode was employed. All electrode potentials were reported with respect to the RHE. The *in situ* STM apparatus used was a Nanoscope E (Digital Instrument Inc.). W tips were electrochemically etched in 0.6 M KOH. IR spectrometer was a Bio-Rad FTS-60A/896 equipped with a liquid N₂-cooled MCT detector. All experiments were carried out in the room temperature of 22-25 °C.

3 RESULTS AND DISCUSSION

3.1 Atomic Structures of Adsorbed Sulfur

3.1.1 Electrochemical measurement

Fig. 1 shows a cyclic voltammogram (CV) of Cu(111) in 0.1 M HClO₄ + 1 mM Na₂S. For comparison, dashed line shows the CV of Cu(111) in pure 0.1 M HClO₄. It is clear that the addition of Na₂S results in a limited double layer potential region. The shape of CV is similar to that obtained in KOH electrolyte, except the potential difference due to different pH of the solutions. The anodic peak commencing at about -0.15 V is attributed to the formation of Cu_xS compound and a cathodic peak at -0.27 V is related to the corresponding reduction. These results strongly suggest that S is chemically adsorbed on Cu(111) surface in the double layer potential region and encourage us to investigate the adlayer structures by using *in situ* STM.

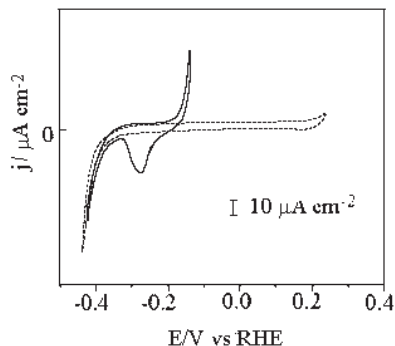


Fig. 1 CV of Cu(111)

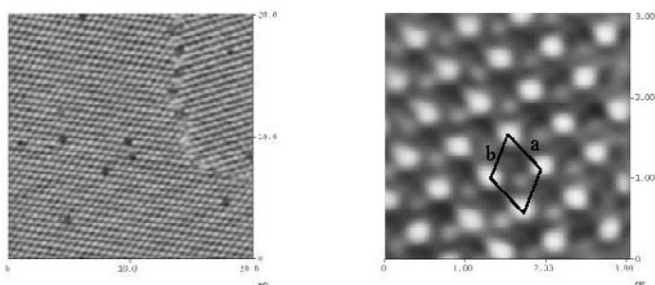


Fig. 2a (left) and b (right) STM images of S on Cu(111)

3.1.2 STM Measurement

After resolving an atomically flat Cu(111) surface and Cu(111)-(1 × 1) structure in HClO₄, drops of Na₂S were directly injected into the STM electrochemical cell. The average concentration of Na₂S in 0.1 M HClO₄ was ca. 1 mM. In situ STM imaging was performed at the potential of -0.32 V positioned in the double layer potential region to avoid the complex formation of Cu_xS. A well-ordered S adlayer was clearly seen after the addition of Na₂S. Fig. 2a is a typical STM image acquired on the S adlayer in a relative large area with mild filtering to delete the imaging noise. The adlayer covers Cu(111) surface and consists of two domains. Several defects appear in the image. The higher resolution STM image shown in Fig. 2b gives us more detailed information of the adlayer structure. According to the periodicity of the S lattice, a unit cell is outlined in Fig. 2b. The interatomic distances in both a and b directions are measured to be 0.66 nm, about $\sqrt{7}$ times of Cu(111) substrate lattice. The atomic rows of S along a and b direction are rotated

by about 19° with respect to the underlying Cu(111)-<110> direction. On the basis of the interatomic distance and orientation, the S adlayer can be defined as a $(\sqrt{7} \times \sqrt{7})R19.1^\circ$ structure. It is seen from Fig. 2b that there are four bright spots at the corner positions and one spot with different brightness at the centroid of one side of the unit cell. Regarding the registry of S atoms with the Cu(111) substrate, a structural model is proposed in Fig. 3. In this model four spots corresponding to the bright spots with high corrugation height in STM images are located on atop sites as iodine on Pt(111), forming the frame of the unit cell. Other two S atoms in the cell are assigned to two 3-fold hollow sites which are related to fcc and hcp position, respectively. This model is similar to the $(\sqrt{7} \times \sqrt{7})R19.1^\circ$ -S on Pd(111) and $(\sqrt{7} \times \sqrt{7})R19.1^\circ$ -I on Pt(111) (Schardt *et al.*, 1989). The so-constructed cell yields a coverage of $3/7$ (ca. 0.43). However, only one S atom in the cell can be resolved in STM image of Fig. 2b, though great effort such as changing tunneling current and bias has been made to obtain high-quality images. In the study of $(\sqrt{7} \times \sqrt{7})R19.1^\circ$ -I adlayer structure on Pt(111) (Schardt *et al.*, 1989), the I on hcp site missed or appeared with a lower corrugation height depending on imaging conditions, while the I adatom on fcc hollow site could be clearly seen in STM image. The apparent height difference between two iodine atoms in hollow sites can be explained as the tunneling probability above an iodine could be lowered by donation of electronic density to the substrate when located directly above a second-layer Pt atom (in the case of hcp I). The corrugation height difference between the two S atoms in hollow sites can be explained as electronic effect due to the second layer of Cu atoms below the surface. The visible spot in STM image corresponds to the S atom in fcc position, and invisible one in hcp position.

The $(\sqrt{7} \times \sqrt{7})R19.1^\circ$ adlayer structure is consistently resolved between potential range from -0.35 V to -0.22 V. Shifting the potential positively more than -0.22 V, a moiré pattern is clearly seen. Fig. 4 is a typical image recorded at -0.20 V. The distance between the two centers of the moiré pattern is measured to be ca. 1.6 nm. More detailed investigations with other surface analysis techniques are needed for intensively understanding the mechanism of the S adsorption as well as the moiré pattern on Cu(111) in solution.

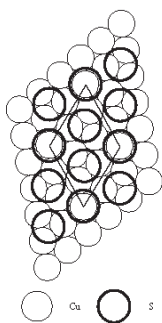


Fig. 3 Structural model of $(\sqrt{7} \times \sqrt{7})R19.1^\circ$

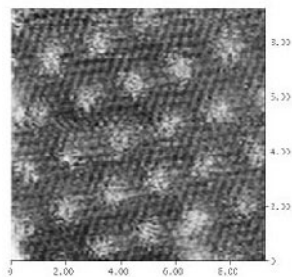


Fig. 4 STM image of moiré pattern

3.2 Controlled Orientation of 2,2'-bipyridine Molecule by Electrode Potentials

The individual bpy molecule was revealed by ECSTM (Wan *et al.*, 2001). Fig. 5a shows a typical STM image of bpy adlayer in a relatively large area acquired at -0.25 V. It is clear that the adlayer is well ordered that only one domain can be seen on a wide terrace even in the negative potential region. The adlayer consists of pairing rows. Two spots in a pair row form an elongated square (Fig. 5a). Each elongated square is assumed to be an individual bpy molecule. A higher resolution STM image in Figure 5b is employed to ascertain the structural details. Each bpy molecule appears in a dumbbell shape with two blobs. The distance between the center of two blobs is ca. 0.4 nm, significantly close to the chemical structure of a bpy molecule. Thus the two blobs are attributed to the two pyridine rings expected from its chemical structure.

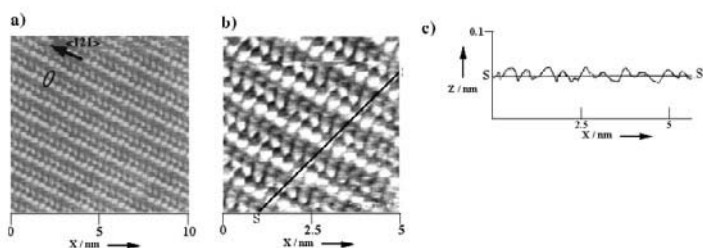


Fig. 5 STM images of bpy

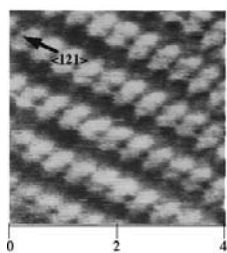


Fig. 6 STM image of bpy

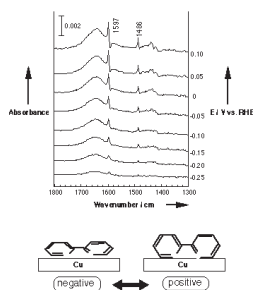


Fig. 7 IR of bpy on Cu(111) in solution

From the feature of STM images in Fig. 5, bpy molecules adsorb on Cu(111) lattice with the two nitrogen atoms in a *cis* form. A careful observation indicates that the corrugation height difference is ca. 0.02 nm in a bpy molecule between two pyridine blobs, showing different contrast in STM images (Fig. 5c). This can be attributed to the molecular torsion from *trans* to *cis* transition. On the other hand, the molecular distance in the same rows along $\langle 12\bar{1} \rangle$ is ca. 0.42 ± 0.2 nm.

The theoretical width of a bpy molecule from N atom to the opposite H atom is ca. 0.4 nm. From STM image and chemical structure, the molecule should orient on Cu(111) in a flat orientation.

The well-ordered adlayer was consistently observed in the negative potential region until -0.4 V where the molecules locally disappeared because of the hydrogen adsorption. On the other hand, it was clearly seen that the molecular orientation varied with scanning electrode potential positively. Fig. 6 is a higher resolution STM image recorded at 0 V, which shows the different molecular feature from that in Fig. 5. The thickness of each molecule is measured to be ca. 0.35 nm. It is reasonable to believe that bpy molecules in Fig. 6 orient vertical on the Cu(111) surface. During the investigation, the constructed bpy adlayer is very stable. After STM imaging for several hours, no damage of the adlayer can be found. And the transition from flat to vertical orientation is completely potential dependent and reversible. The molecule behaves like a reliable electronic element. On the basis of the intermolecular distances and the directions of molecular rows to the underlying Cu(111) lattice measured in STM images, the adlayer is in a $(\sqrt{3} \times \sqrt{3})R76.1^\circ$ symmetry.

A SEIRAS measurement was also carried out to determine the controlled orientation (Fig. 7). The two bands of 1597 and 1486 cm^{-1} are assigned to the adsorbed bpy. It is clearly seen from Fig. 7 that no corresponded peak appears at the potential more negative than -0.25 V, indicating a flat orientation. With shifting electrode potential positively, the peaks emerge with increasing intensities. At 0.1 V the intensity reaches maxim and keep consistent until 0.3 V, indicating that the molecule takes a vertical orientation. The process is completely reversible in both orientation and intensity with applied potential. The molecular states from flat to vertical with the applied potentials are schematically described in the lower part of Fig. 7.

3.3 Controlled Orientation of 1,3,5-triazine-2,4,6-trithiol Molecules

1,3,5-triazine-2,4,6-trithiol has been used as a corrosion resistant for copper and its alloys. The chemical structure of this molecule is described in Fig. 8. The reason that the molecule is chosen as a candidate is due to its characteristic propeller conformation, which is easy to be distinguished in its orientation flat and vertical when it adsorbs on Cu(111).

Fig. 8a is a typical high resolution STM image of 1,3,5-triazine-2,4,6-trithiol adlayer acquired at -0.35 V. It is surprising to see that the STM image shows a distinctly characteristic, propeller-like feature for each molecule with highly ordered arrays, indicating a flat orientation. The molecular rows cross each other at an angle of either 60° or 120° . The molecular distance is measured to be 0.78 ± 0.02 nm, resulting in a (3×3) symmetry. A schematic illustration in the right of Fig. 8a is used to describe the molecular state.

The same molecular arrangement as shown in Fig. 8a was consistently observed in the potential range between -0.35 and -0.1 V. On the other hand, it was found that the molecular orientation changed at positive potentials. A positive potential

step from -0.35 to -0.05 V induced an orientational transition. The STM image in Fig. 8b reveals the orientational variation. Instead of the propeller-like feature, bright spots appear in the STM image. On the basis of the intermolecular distance and the relationship to underlying Cu(111) lattice, the adlayer is still in a (3 x 3) symmetry. The disappearance of the propeller-like feature is attributed to the orientational transition of trithiol molecules. One bright spot corresponds to one trithiol molecule. If the molecules take vertical orientation on Cu(111), only can the top part of the molecules be seen. The proposed model in the right of Fig. 8b shows a side view for the molecule adsorption. The adlayer is stable in the present system. The orientation transition is reversible similar to that in bpy adlayer.

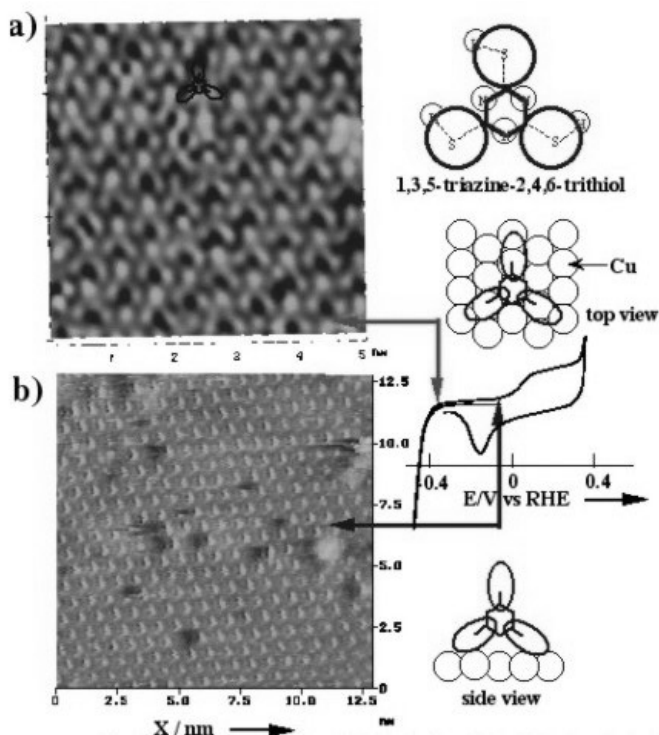


Fig. 8 STM image and CV of 1,3,5-triazine-2,4,6-trithiol molecules

In conclusion, the molecule orientation and structure can be controlled by applying an electrode potential in electrolyte solution and the formation process can be monitored by electrochemical scanning tunneling microscopy. This study should have provided a potential component and insight into molecular electric device fabricated by electrochemical technique although the efforts have to be continuously made for their industrial application, which emphasized the importance of electrochemical techniques in nanoscience and technology.

REFERENCES

- Eigler, D. M., Lutz, C. P. and Rudge, W. E., 1991, An atomic switch realized with the scanning tunneling microscope. *Nature*, **352**, pp. 600-603.
- Eigler, D. M. and Schweizer, E. K., 1990, Positioning single atoms with a scanning tunneling microscope. *Nature*, **344**, pp. 524-526.
- Fishlock, T. W., Oral, A., Egdell, R. G. and Pethica, J. B., 2000, Manipulation of atoms across a surface at room temperature. *Nature*, **404**, pp. 743-745.
- Gimzewski, J. K., Joachim, C., Schlittler, R. R., Langlais, V., Tang, H. and Johannsen, I., 1998, Rotation of a Single Molecule within a Supramolecular Bearing. *Science*, **281**, pp. 531-533.
- Itaya, K., 1998, In situ scanning tunneling microscopy in electrolyte solutions. *Prog. Surf. Sci.*, **58**, pp. 121-247.
- Jung, T. A., Schlittler, R. R. and Gimzewski, J. K., 1997, Conformational identification of individual adsorbed molecules with the STM. *Nature*, **386**, pp. 696-698.
- Jung, T. A., Schlittler, R. R., Gimzewski, J. K., Tang, H. and Joachim, C., 1996, Controlled Room-Temperature Positioning of Individual Molecules: Molecular Flexure and Motion. *Science*, **271**, pp. 181-184.
- Schardt, B. C., Yau, S.-L. and Rinaldi, F., 1989, Atomic Resolution Imaging of Adsorbates on Metal Surfaces in Air: Iodine Adsorption on Pt (111). *Science*, **243**, pp. 1050-1053.
- Stroschio, J. A. and Eigler, D. M., 1991, Atomic and Molecular Manipulation with the Scanning Tunneling Microscope. *Science*, **254**, pp. 1319-1326.
- Whiteside, G. M., Mathias, J. P. and Seto, C. T., 1991, Molecular Self-Assembly and Nanochemistry: A Chemistry Strategy for the Synthesis of Nanostructures. *Science*, **254**, pp. 1312-1319.
- Wan, L. J., Noda, H., Wang, C., Bai, C. L. and Osawa, M., 2001, Controlled Orientation of Individual Molecules by Electrode Potentials. *Chem. Phys.*, **2**, pp. 617-619.